

RLSynC: Offline-Online Reinforcement Learning for Synthon Completion

Frazier N. Baker¹, Ziqi Chen¹, and Xia Ning^{1,2,3}

¹Computer Science and Engineering, The Ohio State University, Columbus, OH

²Translational Data Analytics Institute, The Ohio State University, Columbus, OH

³Biomedical Informatics, The Ohio State University, Columbus, OH

Abstract—Retrosynthesis is the process of determining the set of reactant molecules that can react to form a desired product. Semi-template-based retrosynthesis methods, which imitate the reverse logic of synthesis reactions, first predict the reaction centers in the products, and then complete the resulting synthons back into reactants. These methods enable necessary interpretability and high practical utility to inform synthesis planning. We develop a new offline-online reinforcement learning method RLSynC for synthon completion in semi-template-based methods. RLSynC assigns one agent to each synthon, all of which complete the synthons by conducting actions step by step in a synchronized fashion. RLSynC learns the policy from both offline training episodes and online interactions which allow RLSynC to explore new reaction spaces. RLSynC uses a forward synthesis model to evaluate the likelihood of the predicted reactants in synthesizing a product, and thus guides the action search. We compare RLSynC with the state-of-the-art retrosynthesis methods. Our experimental results demonstrate that RLSynC can outperform these methods with improvement as high as 14.9% on synthon completion, and 14.0% on retrosynthesis, highlighting its potential in synthesis planning.

Index Terms—reinforcement learning, retrosynthesis, multi-agent, synthon completion

I. INTRODUCTION

Retrosynthesis is the process of determining the set of reactant molecules that can react to form a desired product molecule. Retrosynthesis is essential to drug discovery, where medicinal chemists seek to identify feasible synthesis reactions for desired molecules (i.e., synthesis planning [1]). The recent development on computational retrosynthesis methods using deep learning [2]–[15] has enabled high-throughput and large-scale prediction for many products, facilitating medicinal chemists to conduct synthesis planning much more efficiently. Among the existing computational retrosynthesis methods, semi-template-based retrosynthesis methods [11]–[15] imitate the reverse logic of synthesis reactions: they first predict the reaction centers in the products, and then transform (complete) the resulting synthons – the molecular structures from splitting the products at the reaction centers, back into reactants. Semi-template-based retrosynthesis methods enable necessary interpretability as to where the reactions happen among the reactants and how the products are synthesized, and thus have high practical utility to inform synthesis planning.

Existing retrosynthesis methods typically train predictive or generative models to transform from products to their reactants, under the supervision of training data with known reactions. The objective during model training is to reproduce the reactions in the training data, and the model performance is evaluated by comparing the predicted reactions of a product against its known reactions. While these models can accurately recover the known reactions for products, they suffer from two issues: (1) they do not have the capability of exploring and learning new reaction patterns not present in the training data; and (2) they do not have the mechanism to enable a more comprehensive evaluation of the predicted reactions – those that are not identical to known reactions may still be viable. These two issues are under-investigated in the literature.

To address these issues, in this manuscript, we develop a new multi-agent reinforcement learning method with offline learning and online data augmentation, denoted as RLSynC, for synthon completion in semi-template-based methods. Fig. 1 presents the overall idea of RLSynC. We focus on semi-template-based methods due to their interpretability, practical utility and state-of-the-art performance [14], [15]. We particularly focus on their synthon completion step, because reaction centers can be predicted very accurately [15], but synthon completion is often more complicated [16].

Specifically, RLSynC assigns one agent to each synthon, all of which complete the synthons by conducting actions step by step in a synchronized fashion. All the agents share the same action selection policy and select the optimal actions with full observation of other agents’ states. RLSynC learns the policy from offline training episodes, and augmented training data generated through online interactions. The augmented data introduce new reaction patterns not included in training data, and thus allow RLSynC to explore new reaction spaces. RLSynC uses a reward function to evaluate the likelihood of the predicted reactants in synthesizing a product, and thus guides the action search. We compare RLSynC with state-of-the-art retrosynthesis methods. Our experimental results demonstrate that RLSynC can outperform these methods with improvement as high as 14.9% on synthon completion, and 14.0% on retrosynthesis. To the best of our knowledge, RLSynC is the first reinforcement learning method for synthon completion.

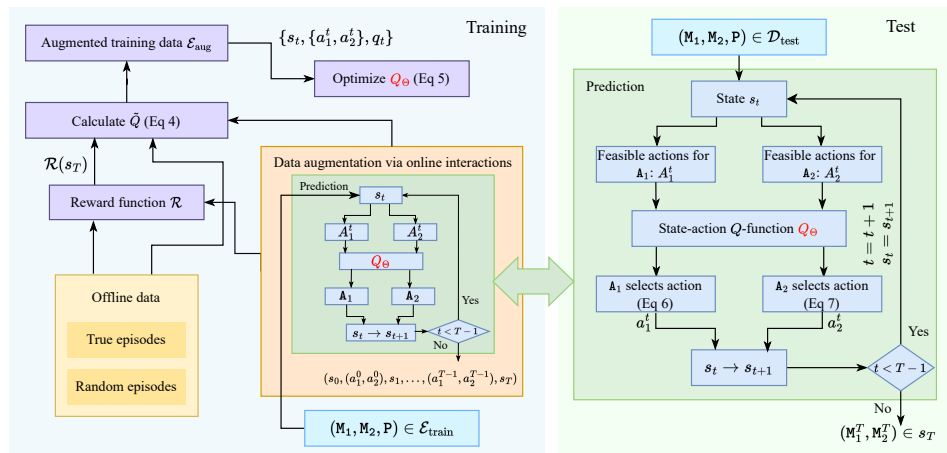


Fig. 1: Overview Scheme of RLSynC

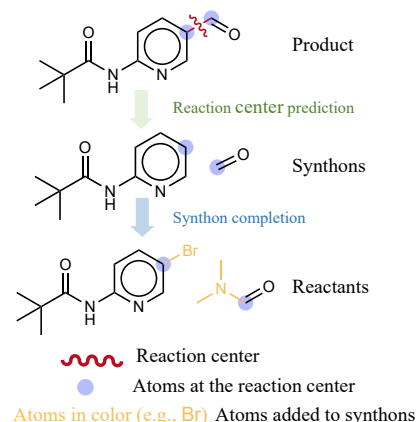


Fig. 2: Retrosynthesis Process

II. RELATED WORK

A. Retrosynthesis

Deep-learning-based retrosynthesis methods can be categorized into three groups: template-based, template-free and semi-template-based. Template-based methods [2]–[5] use reaction templates that are extracted from known reactions to transform a product directly into reactants, and thus are limited to reactions covered by the templates. Template-free methods [6]–[10] typically utilize the sequence representation of molecules (SMILES) and employ Transformer models to translate product SMILES strings into reactant SMILES strings, without using reaction templates. For example, RSMILES [9] uses a Transformer to decode the reactant SMILES strings from the product SMILES strings. RetroFormer [10] embeds both the SMILES strings and molecular graphs of products, and uses the embeddings to predict reaction center regions and generate reactant SMILES strings. However, these methods may generate SMILES strings that violate SMILES grammars or chemical rules.

Semi-template-based methods [11]–[15] have two steps: (1) they first identify the reaction centers and break the product into synthons using reaction centers; and then (2) they complete synthons into reactants. For example, RetroPrime [13] employs two Transformers to first translate the SMILES strings of products to synthons, and then synthons to reactants. GraphRetro [14] predicts reaction centers by learning from the molecular graphs of products, and then completes synthons by classifying the subgraphs based on whether they can realize the difference between synthons and reactants. G²Retro [15] also predicts reaction centers from molecular graphs, and then completes synthons by sequentially adding rings or bonds.

B. Reinforcement Learning

Deep reinforcement learning methods have been developed to design new small molecules. For example, GCPN [17] uses a graph convolutional policy network to sequentially add new atoms and bonds to construct new molecules. MolDQN [18] uses Morgan fingerprints [19] to represent molecules, and

learns a deep Q-network to guide the addition or change of atoms and bonds, modifying molecules to have desired properties. Reinforcement learning has also been applied for biological sequence design. For example, DyNA PPO [20] uses a model-based variant of proximal-policy optimization to generate DNA and peptide sequences with desired properties. TCRPPO [21] learns a mutation policy to mutate sequences of T-cell receptors to recognize specific peptides.

Reinforcement learning has been used for multi-step retrosynthetic planning, which seeks to find an optimal sequence of multiple reactions to synthesize a product. Schreck *et al.* [22] trains an agent to select reactions from a list to construct the sequence backward starting from the product, until all the reactants of the first reaction in the sequence are purchasable. In this method, reinforcement learning is used to select reactions rather than predicting reactions. However, there is very limited work applying reinforcement learning to retrosynthesis. RCSearcher [23] applies a deep Q network to search a molecular graph for reaction centers. In contrast, RLSynC uses reinforcement learning for synthon completion.

III. DEFINITIONS AND NOTATIONS

A synthesis reaction involves a set of reactants $\{R_i\}$ and a product molecule P that is synthesized from these reactants. Each reactant R_i has a corresponding synthon M_i , which represents the substructures of R_i that appear in P . The connection point of these synthons to form the product, typically a bond, is referred to as the reaction center. Fig. 2 presents the retrosynthesis process. In retrosynthesis, a typical semi-template-based method first identifies the reaction center and thus the corresponding synthons $\{M_i\}$, and then completes the synthons back to reactants $\{R_i\}$.

To complete M_i to R_i , atoms may be added to M_i one at a time, through establishing new bonds. In each step t , the intermediate molecular structure generated from M_i is denoted as M_i^t . With abuse of terms, such intermediate molecular structures are referred to as *current* synthons. In this manuscript, we focus on the reactions with only two reactants, because

TABLE I: Key Notations

Notation	Meaning
P	product molecule
(R_1, R_2)	a pair of reactants
(M_1, M_2)	a pair of synthons
(M_1^t, M_2^t)	a pair of <i>current</i> synthons at step t
A	an agent
t/T	time step/time step limit
MDP	Markov decision process: $\text{MDP} = \{\mathcal{S}, \mathcal{A}, \mathcal{T}, \mathcal{R}\}$
\mathcal{S}/s_t	State space/a state at step t
$\mathcal{A}/a_1^t/a_2^t$	Action space/an action used to update M_1^t/M_2^t at step t
A_i^t	the set of feasible actions for A_i at time step t
\mathcal{T}	State transition function
$\mathcal{R}(s_T)$	reward function for terminal states

this is the most common case in synthesis reactions [16]. For example, in the USPTO-50K benchmark dataset [11], two-reactant synthesis reactions take 70.8%. In this manuscript, the two terms ‘‘pair of reactants’’ and ‘‘reaction’’ for a product are used interchangeably, when no ambiguity is raised; the term ‘‘prediction’’ refers to the prediction of the two reactants of a product. Table I presents the key definitions and notations.

RLSynC is employed under the assumption that reaction centers are pre-determined or can be accurately predicted. This is because the potential reaction centers are typically limited, especially in the case of small molecules. According to Chen *et.al.* [15], reaction center prediction can achieve as high as 97.2% accuracy. However, synthon completion is often more complicated and can be realized in a variety of ways [16]. However, RLSynC can be generalized to one-reactant (29.0% in the USPTO-50K benchmark dataset) or multi-reactant (0.2% in USPTO-50K) cases by having one or multiple agents, given how RLSynC completes synthons (Section V).

IV. RLSynC MODEL

RLSynC assigns one agent, denoted as A, to each synthon and uses the agent to transform its synthon into a reactant through a sequence of actions. This transformation is achieved through a Markov Decision Process (MDP), denoted as $\text{MDP} = \{\mathcal{S}, \mathcal{A}, \mathcal{T}, \mathcal{R}\}$, including a state space \mathcal{S} , an action space \mathcal{A} , a transition function \mathcal{T} and a reward function \mathcal{R} .

A. State Space (\mathcal{S})

RLSynC has a discrete state space \mathcal{S} describing the MDP status. Each state $s_t \in \mathcal{S}$ is represented as:

$$s_{t,P} = \{M_1, M_2, M_1^t, M_2^t, P, T - t\}, \quad (1)$$

where t denotes the steps of actions (Section IV-B); M_1 and M_2 are the synthons from P that are assigned to agent A_1 and A_2 , respectively; M_1^t and M_2^t are the *current* synthons generated from M_1 and M_2 after t ($t = 0, \dots, T$) steps of actions by A_1 and A_2 , respectively ($M_1^0 = M_1, M_2^0 = M_2$); P is the product molecule; and T is the step limit and thus s_T is a terminal state. The current synthons (M_1^T, M_2^T) in s_T are the predicted reactants. In RLSynC, T is set to 3 because 89.10% of the synthons in the benchmark USPTO-50K dataset can be completed with the addition of up to 3 atoms. Empirically, increasing T could

decrease model performance, without significantly increasing coverage over reactions (e.g., $T = 6$ will cover only an additional 2.96% of the synthons in the benchmark dataset). When no ambiguity is raised, $s_{t,P}$ is represented as s_t with P dropped.

B. Action Space (\mathcal{A})

RLSynC has two types of actions in its action space \mathcal{A} : (1) adding atoms via bonds, denoted as ADD, and (2) no operation (i.e., doing nothing), denoted as NOOP. For ADD, RLSynC allows 12 types of atoms (B, C, N, O, F, Si, P, S, Cl, Se, Br, and I) via single, double or triple bonds, and thus 36 types of additions. These additions are sufficient to complete 98.42% of the synthons in those two-synthon cases in the benchmark data within 3 steps. Adding more atom and bond types offers very little additional coverage. but expands the action space. Thus, the action space is denoted as follows:

$$\mathcal{A} = \{\text{ADD}_1, \text{ADD}_2, \dots, \text{ADD}_{36}, \text{NOOP}\}, \quad (2)$$

where each ADD_i corresponds to a specific atom type and bond type combination. The atom additions have to satisfy the following constraints:

- The new atoms are only added to the reaction centers or atoms that are added through the previous actions;
- The bonds connecting the new added atoms and the current synthons do not violate structural or valency rules;
- The types of these new bonds exist in the training data.

At each step t ($t = 0, \dots, T$), each agent A_i selects an action a_i^t from \mathcal{A} , and applies the action to its current synthon M_i^t ($i=1, 2$). The two agents act in a synchronized fashion and start the next step $t+1$ only when both finish step t . Note that each agent at step t has perfect observations of its own action and current synthon, and also the other agent’s current synthon. This full observation allows the agents to share the same policy without exchanging information, and thus simplifies the policy learning (Section V-C).

C. Transition Function (\mathcal{T})

The transition function $\mathcal{T}(s_{t+1}|s_t, \{a_1^t, a_2^t\})$ in RLSynC calculates the probability of MDP transitioning to state s_{t+1} , given the current state s_t and actions $\{a_1^t, a_2^t\}$ at step t . In RLSynC, \mathcal{T} is deterministic, that is, $\mathcal{T}(s_{t+1}|s_t, \{a_1^t, a_2^t\}) = 1$.

D. Reward Function (\mathcal{R})

RLSynC uses a final binary reward to guide its agents. At the terminal step T , if the predicted reactants M_1^T and M_2^T exactly match the reactants given for the product P in the training data, \mathcal{R} gives s_T a reward 1. Otherwise, a stand-alone forward synthesis prediction model is applied to predict the products that can be synthesized from M_1^T and M_2^T . If P is among the top-5 predictions by this model, \mathcal{R} gives s_T a reward 1; otherwise, reward 0. RLSynC uses Molecular Transformer [24] as the forward synthesis prediction model, because it is the state of the art and achieves very high accuracy for forward synthesis prediction [25]. However, RLSynC is not bound to Molecular Transformer and can be easily adapted to any other forward

synthesis prediction models for \mathcal{R} . Predicted reactants that receive positive rewards are referred to as *correct* predictions.

E. State-Action Representation

The state-action pairs will be used to learn a state-action Q-value function (discussed later in Section V-A). RLSynC represents a state-action pair $(\mathbf{s}_t, \{\mathbf{a}_1^t, \mathbf{a}_2^t\})$ as follows:

$$\mathbf{h}_{i,t} = \mathbf{m}_i \oplus \mathbf{m}_j \oplus \mathbf{m}_i^{t+1} \oplus \mathbf{m}_j^{t+1} \oplus \mathbf{p} \oplus [T - (t + 1)], \quad (3)$$

where $i = 1, 2$ indexing the agent of interest, $j = 3 - i$ indexing the other agent; \mathbf{m} 's are the Morgan fingerprint vectors for the corresponding synthons \mathbf{M} 's (\mathbf{M}_i^t will be transformed to \mathbf{M}_i^{t+1} by \mathbf{a}_i^t , and \mathbf{M}_i^{t+1} is represented by \mathbf{m}_i^{t+1}); \mathbf{p} is the Morgan fingerprint vector for the product \mathbf{P} ; and \oplus is the concatenation operation. The use of Morgan fingerprints is inspired by Zhou *et.al.* [18]. Morgan fingerprints [19] capture molecular substructure information, are easy to construct and do not require representation learning.

V. RLSynC TRAINING AND PREDICTION

A. Offline Training

At a state $\mathbf{s}_t = \{\mathbf{M}_1, \mathbf{M}_2, \mathbf{M}_1^t, \mathbf{M}_2^t, \mathbf{P}, T - t\}$, RLSynC uses a state-action value function $Q_\Theta(\mathbf{s}_t, \{\mathbf{a}_1^t, \mathbf{a}_2^t\})$, parameterized by Θ , to estimate the future rewards of \mathbf{s}_t if the actions \mathbf{a}_1^t and \mathbf{a}_2^t are applied by \mathbf{A}_1 and \mathbf{A}_2 on \mathbf{M}_1^t and \mathbf{M}_2^t , respectively. $Q_\Theta(\mathbf{s}_t, \{\mathbf{a}_1^t, \mathbf{a}_2^t\})$ is modeled as a multi-layer fully-connected neural network, with $(\mathbf{s}_t, \{\mathbf{a}_1^t, \mathbf{a}_2^t\})$ represented as $\mathbf{h}_{i,t}$ (Equation 3) as input to the neural network.

1) *Offline Training Episode Generation:* To learn Q_Θ , RLSynC uses offline data of pre-computed episodes. An episode refers to a trajectory from \mathbf{s}_0 to \mathbf{s}_T for a product \mathbf{P} , that is, $(\mathbf{s}_0, \{\mathbf{a}_1^0, \mathbf{a}_2^0\}, \mathbf{s}_1, \{\mathbf{a}_1^1, \mathbf{a}_2^1\}, \mathbf{s}_2, \dots, \{\mathbf{a}_1^{T-1}, \mathbf{a}_2^{T-1}\}, \mathbf{s}_T, \mathcal{R}(\mathbf{s}_T))_{\mathbf{P}}$. RLSynC computes all *true* episodes from training data that include known reactions to synthesize given products. For each product in the training set, RLSynC also computes 4 *random* episodes from a set of random reactions that are not included in the training data. These random reactions are generated by taking random actions on the synthons of the products in the training data, and their rewards are calculated using \mathcal{R} . While all the *true* episodes for known reactions have positive rewards, most episodes for random reactions have zero rewards. By training on both positive- and zero-reward episodes, the agents can learn actions to take as well as actions to avoid, thereby improving their overall performance.

2) *Q-Value Function Learning:* From the offline training episodes, RLSynC uses a SARSA [26]-like approach to approximate the Q-value $\tilde{Q}(\mathbf{s}_t, \{\mathbf{a}_1^t, \mathbf{a}_2^t\})$ as follows:

$$\tilde{Q}(\mathbf{s}_t, \{\mathbf{a}_1^t, \mathbf{a}_2^t\}) = \begin{cases} \gamma \tilde{Q}(\mathbf{s}_{t+1}, \{\mathbf{a}_1^{t+1}, \mathbf{a}_2^{t+1}\}) & \text{if } t < T-1, \\ \mathcal{R}(\mathbf{s}_{t+1}) & \text{if } t = T-1, \end{cases} \quad (4)$$

where $0 < \gamma < 1$ is the discount factor and \mathcal{R} is the reward function. With the approximate Q-values, RLSynC

learns $Q_\Theta(\mathbf{s}_t, \{\mathbf{a}_1^t, \mathbf{a}_2^t\})$ by minimizing the following loss function:

$$\mathcal{L}(\Theta|\mathcal{E}) = \frac{1}{|\mathcal{E}|} \sum_{\{\mathbf{s}_t, \{\mathbf{a}_1^t, \mathbf{a}_2^t\}\} \in \mathcal{E}} (Q_\Theta(\mathbf{s}_t, \{\mathbf{a}_1^t, \mathbf{a}_2^t\}) - q_t)^2 + \alpha \mathcal{R}_{\ell_2}(\Theta), \quad (5)$$

where \mathcal{E} is the set of all $\{\mathbf{s}_t, \{\mathbf{a}_1^t, \mathbf{a}_2^t\}\}$ pairs from the offline training episodes and $|\mathcal{E}|$ is its size; $q_t = \tilde{Q}(\mathbf{s}_t, \{\mathbf{a}_1^t, \mathbf{a}_2^t\})$ is calculated from Equation 4; \mathcal{R}_{ℓ_2} is the ℓ_2 -norm regularizer over Θ ; and $\alpha > 0$ is a trade-off parameter.

B. Training Data Augmentation via Online Interactions

The offline training has the advantage of sourcing experience from known reactions, and thus exposing RLSynC to successful synthon completion patterns (i.e., the *true* episodes). However, it also eliminates the opportunity for RLSynC to explore and discover new synthon completion patterns that are not included in the training data. To mitigate this issue, inspired by Schneider *et.al.* [27], RLSynC deploys an innovative strategy to augment the offline training data via online interactions, denoted as RLSynC-aug.

1) Augmentation through Greedy Action Selection:

RLSynC first learns Q_Θ using the known and random reactions as discussed above (Section V-A). The optimized agents are then applied to the original unaugmented training data (only known reactions, excluding random reactions), and generate one new episode for each unique product in the training data from the actions they take and the rewards the actions receive (action selection discussed later in Section V-C). These new episodes are added to and augment the training data. Q_Θ is then re-learned from this new augmented training data and the new agents generate another set of new episodes for further training data augmentation. The above process is iterated until the performance of the agents on the separate validation set is not improved.

2) *Augmentation through Top-N Prediction Search:* Once the agents' performance is stabilized, a more aggressive strategy is deployed to generate additional new episodes through top- N prediction search (discussed later in Section V-D) and tracking back the episodes leading to the top- N predictions, resulting in N episodes for each product. Multiple iterations of such top- N -prediction-based new episode generation are conducted and training data is augmented until validation set performance ceases to improve. A final Q_Θ will be learned over the final augmented training data.

Augmenting the training data with additional positive-reward episodes exposes RLSynC to new reactions that do not exist in the training data, thus allowing RLSynC to explore beyond the limits of the data. Augmenting the training data with additional zero-reward episodes helps RLSynC correct inaccurate Q-value estimations, enhancing its robustness and effectiveness. Algorithm 1 presents RLSynC-aug.

C. Action Selection Policy

In predicting the reactants of a new product \mathbf{P} (i.e., in validation set or test set), the agents of RLSynC predict and select actions to complete synthons via up to T steps. To

Algorithm 1 RLSynC-aug

Input: $\mathcal{E}_{\text{train}}, \mathcal{E}_{\text{random}}, \mathcal{D}_{\text{validation}}, k, N$ **Output:** Q_{Θ^*}

```
1:  $\mathcal{E}_{\text{aug}} = \mathcal{E}_{\text{train}} \cup \mathcal{E}_{\text{random}}$  { $\mathcal{E}$  refers to the set of episodes}
2:  $\mathcal{E}_{\text{aug}}^* = \mathcal{E}_{\text{aug}}$ 
3:  $\Theta = \arg \min_{\Theta} \mathcal{L}(\Theta | \mathcal{E}_{\text{aug}}^*)$  {Equation 5}
4:  $\text{map}^* = -1, \text{flag} = 0$ 
5:  $\text{map} = \text{MAP}@N(Q_{\Theta}, \mathcal{D}_{\text{validation}})$  {Equation 8}
6: while  $\text{map} > \text{map}^*$  do
7:    $\text{map}^* = \text{map}, \Theta^* = \Theta, \mathcal{E}_{\text{aug}} = \mathcal{E}_{\text{aug}}^*$ 
8:   for all  $P$  in  $\mathcal{E}_{\text{train}}$  do
9:     if  $\text{flag} == 0$  then
10:       $\mathcal{E}_{\text{aug}}^* = \mathcal{E}_{\text{aug}} \cup \text{RLSynC-search}(M_1, M_2, P, T, 1, 1, Q_{\Theta})$ 
11:    else
12:       $\mathcal{E}_{\text{aug}}^* = \mathcal{E}_{\text{aug}} \cup \text{RLSynC-search}(M_1, M_2, P, T, k, N, Q_{\Theta})$ 
13:    end if
14:  end for
15:   $\Theta = \arg \min_{\Theta} \mathcal{L}(\Theta | \mathcal{E}_{\text{aug}}^*)$  {Equation 5}
16:   $\text{map} = \text{MAP}@N(Q_{\Theta}, \mathcal{D}_{\text{validation}})$  {Equation 8}
17:  if  $\text{map} \leq \text{map}^*$  and  $\text{flag} == 0$  then
18:     $\text{flag} = 1, \text{map}^* = -1, \Theta = \Theta^*, \mathcal{E}_{\text{aug}}^* = \mathcal{E}_{\text{aug}}$ 
19:  end if
20: end while
21: return  $Q_{\Theta^*}$ 
```

predict the action \mathbf{a}_i^t for agent A_i at time t , RLSynC first identifies the set of all chemically feasible atom additions, denoted as A_i^t ($A_i^t \subseteq \mathcal{A}$), for M_i^t satisfying the constraints as in Section IV-B. A_i samples the best action $\mathbf{a}_i^t \in A_i^t$ ($i = 1, 2$) if the action has the maximum predicted Q -value, as follows:

$$\mathbf{a}_1^t = \arg \max_{\mathbf{a} \in A_1^t} Q_{\Theta}(\mathbf{s}_t, \{\mathbf{a}, \text{NOOP}\}), \quad (6)$$

$$\mathbf{a}_2^t = \arg \max_{\mathbf{a} \in A_2^t} Q_{\Theta}(\mathbf{s}_t, \{\text{NOOP}, \mathbf{a}\}). \quad (7)$$

That is, each agent assumes NOOP from the other agent, but observes the other agent’s *current* synthon in \mathbf{s}_t in order to select its next optimal action. Please note that the two agents share the same Q_{Θ} function and follow the same policy.

D. Top- N Prediction Search

RLSynC uses a novel greedy search algorithm, denoted as RLSynC-search, to identify the top- N predicted reactions with the highest Q -values. In training data augmentation, such top- N pairs will be used to augment the training data (Section V-B2). In predicting reactants for new products (e.g., in test set), the top- N predictions provide more options for synthesis planning. Specially, at step $t = 0$, instead of selecting only one action, each agent selects k actions with the top- k highest Q -values calculated based on Equation 6 and 7 (i.e., instead of “max” in Equation 6 and 7, use “top- k ”). Thus, there will be k^2 possible next states, resulting from all possible action combinations from the two agents. In each of the possible next states, each agent selects again k actions for its current synthon. Through T steps, this process will result in k^{2T} predicted reactions at the terminal state. RLSynC sorts

Algorithm 2 RLSynC-search

Input: $M_1, M_2, P, T, k, N, Q_{\Theta}$ **Output:** Top- N predictions $\mathcal{E}_{\text{top-}N}$

```
1:  $M_1^0 = M_1, M_2^0 = M_2$ 
2:  $s_0 = \{M_1, M_2, M_1^0, M_2^0, P, T\}, \mathbb{S}_0 = \{s_0\}$ 
3: for  $t = 1$  to  $T$  do
4:    $\mathbb{S}_t = \emptyset$ 
5:   for all  $s_{t-1} \in \mathbb{S}_{t-1}$  do
6:     for all agent  $A_i$  ( $i = 1, 2$ ) do
7:        $V_i = \emptyset$ 
8:       for all  $\mathbf{a} \in A_i^{t-1}$  do
9:          $V_i = V_i \cup \{(a : Q_{\Theta}(s_{t-1}, \{\mathbf{a}, \text{NOOP}\}))\}$  {or
            $\{\text{NOOP}, \mathbf{a}\}, \text{Equation 4}$ }
10:      end for
11:       $V_i = \text{sorted}(V_i, \text{'decreasing'})[1:k]$ 
12:    end for
13:    for all  $\{\mathbf{a}_1^{t-1}, \mathbf{a}_2^{t-1}\} \in V_1 \times V_2$  do
14:      identify  $s_t$  s.t.  $\mathcal{T}(s_t | s_{t-1}, \{\mathbf{a}_1^{t-1}, \mathbf{a}_2^{t-1}\}) = 1$ 
15:       $q_t = Q_{\Theta}(s_{t-1}, \{\mathbf{a}_1^{t-1}, \mathbf{a}_2^{t-1}\})$ 
16:       $\mathbb{S}_t = \mathbb{S}_t \cup \{(\{\mathbf{a}_1^{t-1}, \mathbf{a}_2^{t-1}\}, s_t) : q_t\}$ 
17:    end for
18:  end for
19: end for
20: return  $\mathcal{E}_{\text{top-}N} = \text{sorted}(\mathbb{S}_T, \text{'decreasing'})[1:N]$ 
```

all these predicted reactions using their Q -values and selects the top- N predictions. While this process can be expensive, the actions on each of the possible next states can be done independently, and this process can be implemented in parallel. The algorithm is presented in Algorithm 2.

VI. EXPERIMENTAL SETTINGS

A. Data

We use the benchmark USPTO-50K dataset [28] in our experiments, which contains 50,016 chemical reactions. We use the same training, validation and testing division as in the literature [11], resulting in 40,008 reactions for training, 5,001 for validation, and 5,007 for testing. From each set, we use only the reactions that satisfy the following constraints:

- The reaction has exactly two reactants;
- The synthons can be completed to the ground-truth reactants by adding no more than three atoms.

After applying the above filter, our training, validation, and test sets contain 25,225, 3,172 and 3,167 reactions, respectively.

B. Baselines

We compare RLSynC against five state-of-the-art retrosynthesis methods: G²Retro [15] and GraphRetro [14] are graph-based methods that complete synthons through the addition of leaving groups. RSMILES [9], RetroPrime [13], and RetroFormer [10] are sequence-based methods that use Transformer models [29] to generate string representations of reactants. Please note that RSMILES offers both template-free and semi-template-based approaches to retrosynthesis.

While we are primarily interested in the semi-template-based approach from RSMILES, we still include results for its template-free approach for completeness. RetroFormer only offers a template-free approach, and all the other methods offer semi-template-based approaches. Note that we do not compare RLSynC against the methods that the above baselines outperform for retrosynthesis [15], or if the methods do not have source code available.

C. Evaluation Metrics

We evaluate different methods in terms of the correctness, diversity and validity of their predicted reactants.

1) *Correctness Metrics*: Two predicted reactants of a product are considered *correct* if they receive reward 1. To measure the correctness of top- N predicted reactant pairs, we use mean average precision at top N (MAP@ N), defined as follows:

$$\text{MAP@}N = \frac{1}{|\mathcal{D}_{\text{test}}|} \sum_{\text{P} \in \mathcal{D}_{\text{test}}} \frac{1}{N} \sum_{k=1}^N \mathcal{R}(\{M_1^T, M_2^T\}_{\text{P},k}), \quad (8)$$

where $\mathcal{D}_{\text{test}}$ is the test set, P is a product in $\mathcal{D}_{\text{test}}$, \mathcal{R} is the reward (Section IV-D), $\{M_1^T, M_2^T\}_{\text{P},k}$ is the k -th ranked predicted reactants (i.e., at the terminal step T , see Section IV-A) for P . Higher MAP@ N indicates better correctness among top- N predictions. Note that MAP@ N is different from accuracy@ N in retrosynthesis prediction [9], [14], [15], which compares the predictions only with the ground-truth reactions.

We also use normalized discounted cumulative gain at top N (NDCG@ N), which is a popular metric in evaluating ranking. In our experiments, NDCG@ N uses the rewards as gains and captures both the rewards and the ranking positions of the predictions. Higher NDCG@ N indicates that correct predictions tend to be ranked higher.

2) *Diversity Metrics*: We also measure the diversity of the correct predictions from different methods. A diverse set of correct predictions enables a broad range of viable options to synthesize a product, and thus is preferred in synthesis planning. We measure diversity using the average pairwise similarity among the top- N correct predictions, as follows:

$$\text{Diversity@}N = 1 - \frac{\sum_{\text{P} \in \mathcal{D}_{\text{test}}} \sum_{j=1}^N \sum_{k=j+1}^N \text{sim}(r_j, r_k)_{\text{P}} \mathcal{R}(r_j)_{\text{P}} \mathcal{R}(r_k)_{\text{P}}}{0.5 \times (N_{\text{P}} - 1) N_{\text{P}}},$$

where r_j is the j -th ranked predicted reactions for P (i.e., $r_j = \{M_1^T, M_2^T\}_{\text{P},j}$); $\mathcal{R}(r_j)_{\text{P}}$ is the reward for r_j (for correct predictions, $\mathcal{R}(r_j)_{\text{P}} = 1$; otherwise 0); $N_{\text{P}} = \sum_{j=1}^N \mathcal{R}(r_j)_{\text{P}}$, that is, it is the number of correct predictions; $\text{sim}(r_j, r_k)_{\text{P}}$ is the similarity between two sets of reactant pairs:

$$\begin{aligned} \text{sim}(r_j, r_k) &= \text{sim}(\{M_{1j}^T, M_{2j}^T\}, \{M_{1k}^T, M_{2k}^T\}) \\ &= \frac{1}{2} \max(\text{sim}_{\text{M}}(M_{1j}^T, M_{1k}^T) + \text{sim}_{\text{M}}(M_{2j}^T, M_{2k}^T), \\ &\quad \text{sim}_{\text{M}}(M_{1j}^T, M_{2k}^T) + \text{sim}_{\text{M}}(M_{2j}^T, M_{1k}^T)), \end{aligned}$$

where M_{ij}^T is the i -th predicted reactant ($i = 1, 2$) for the j -th product; sim_{M} is the Tanimoto similarity [30] between two reactants.

3) *Validity*: We consider a predicted reaction to be valid if both the SMILES strings for the predicted reactants are valid. Valid SMILES strings should obey standard valency rules. Validity at top N is calculated as the percentage of valid predictions among all the top- N predictions.

VII. EXPERIMENTAL RESULTS

We first compare RLSynC directly to the synthon completion components of the baselines by providing known reaction centers to all the methods. We further examine the performance of RLSynC using predicted reaction centers against the baselines for retrosynthesis.

A. Evaluation on Synthon Completion

TABLE II: MAP@ N of Synthon Completion

N	1	2	3	4	5	6	7	8	9	10
RSMILES	0.953	0.863	0.795	0.734	0.681	0.636	0.601	0.571	0.545	0.523
GraphRetro	<u>0.912</u>	0.861	0.827	0.804	0.779	0.747	0.715	0.687	0.662	0.643
G ² Retro	0.950	0.893	0.855	0.823	0.789	0.753	0.720	0.691	0.665	0.645
RLSynC	0.927	0.898	0.874	0.845	0.822	0.803	0.784	0.769	0.754	0.741
imprv.(%)	-2.7*	0.6	2.2*	2.7*	4.2*	6.6*	8.9*	11.3*	13.4*	14.9*

The best performance for each N is in **bold**, and the best performance among the baseline method is underlined. The row ‘imprv.’ presents the percentage improvement of RLSynC over the best-performing baseline methods (underlined). The * indicates that the improvement is statistically significant at 95% confidence level.

TABLE III: NDCG@ N for Synthon Completion

N	1	2	3	4	5	6	7	8	9	10
RSMILES	0.953	0.883	0.831	0.784	0.742	0.707	0.678	0.652	0.630	0.611
GraphRetro	<u>0.912</u>	0.872	0.846	0.827	0.807	0.784	0.760	0.739	0.719	0.703
G ² Retro	0.950	0.905	0.876	0.851	0.825	0.798	0.773	0.750	0.729	0.712
RLSynC	0.927	0.905	0.886	0.865	0.847	0.832	0.817	0.805	0.793	0.782
imprv.(%)	-2.7*	0.0	1.1*	1.6*	2.7*	4.3*	5.7*	7.3*	8.8*	9.8*

The annotations in this table are the same as those in Table II.

1) *Correctness Evaluation*: Table II and Table III present the performance of all the methods in terms of MAP@ N and NDCG@ N . As Table II shows, in terms of MAP@ N , RLSynC outperforms the baseline methods consistently for $N \in [2, 10]$. G²Retro is the best baseline, with the best MAP@ N among all baselines at $N \in [2, 10]$, and very close to the best MAP@1. RLSynC significantly outperforms G²Retro on 8 results, with the best improvement 14.9% at $N = 10$ and average improvement 7.2% over $N \in [2, 10]$, with 8 improvements statistically significant. As N increases, the performance improvement from RLSynC over other methods also increases, indicating that RLSynC generates more positive-reward reactions than other methods among top- N predictions. This capability of RLSynC could facilitate the design of multiple synthesis reactions in synthesis planning. Note that as N increases, top- N predictions tend to include more incorrect predictions, leading to a decrease in MAP@ N .

G²Retro completes synthons into reactants by sequentially attaching substructures (i.e., bonds or rings) starting from the reaction centers. Unlike G²Retro, which exclusively learns

from known reactions, RLSynC benefits from random reactions and online iterations of augmented data, therefore, it can overcome the potential limitations and biases in the known reactions. In addition, RLSynC can adapt and improve from past mistakes by learning from online iterations of data augmentation, and thus correct inaccurate Q -value predictions in zero-reward episodes. These advantages enable RLSynC to finally outperform G^2 Retro.

RSMILES employs a Transformer model to translate root-aligned synthon SMILES strings into reactant strings. It also augments the training and test synthon SMILES strings with varied atom orders to further improve the performance. However, RSMILES is trained to recover the unique SMILES strings of ground-truth reactants from the training data, disregarding other possible reactants to synthesize the same product. In contrast, by augmenting data with the online interactions, particularly through top- N search, RLSynC focuses beyond just the top-1 prediction and aims to maximize the rewards for the overall top- N predictions. As a result, RLSynC achieves better MAP@ N for $N \in [2, 10]$ than RSMILES. GraphRetro formulates synthon completion as a classification problem over subgraphs. However, it ignores the impact of predicted subgraphs on the overall structures of resulting reactants, which may lead to incorrect predictions. Unlike GraphRetro, RLSynC predicts reactants by adding feasible bonds and atoms to *current* synthons under the guidance of rewards for resulting molecules. As a result, RLSynC outperforms GraphRetro on MAP@ N at $N \in [1, 10]$.

Similar trends can be observed in Table III: in terms of NDCG@ N , RLSynC consistently outperforms the best baseline method G^2 Retro at $N \in [3, 10]$, all with statistically significant improvement; the best improvement is 9.8% at $N = 10$, and average improvement 5.2% over $N \in [3, 10]$. RLSynC achieves the same performance as G^2 Retro at $N = 2$. RSMILES achieves the best NDCG@1 performance among all the methods, but its performance dramatically decreases for larger N . GraphRetro’s performance is between G^2 Retro and RSMILES. The difference between MAP@ N and NDCG@ N is that NDCG@ N discounts the impact of low-ranking correct predictions. The fact that RLSynC achieves both high MAP@ N and NDCG@ N indicates that RLSynC predicts more correct reactions at high ranks (e.g., top-2, top-3).

2) *Diversity Evaluation*: Table IV presents the performance of different methods in terms of Diversity@ N among their correct predictions. Similar trends to those for MAP@ N and NDCG@ N can be observed for Diversity@ N . RLSynC outperforms the best baselines, GraphRetro and G^2 Retro at $N \in [4, 10]$, all with statistical significance, with the best improvement 13.1% at $N = 6$, and average improvement 10.6% over $N \in [4, 10]$. RLSynC ties with GraphRetro for best Diversity@3 performance, and only slightly underperforms G^2 Retro at $N = 1$ with no statistical significance.

While all the baseline methods are limited by the synthon completion patterns within known reactions from the training data, RLSynC is able to discover patterns not present in the training data by learning from augmented data via online

interactions. These newly discovered patterns could contribute to the better Diversity@ N at $N \in [3, 10]$ for RLSynC. Higher Diversity@ N indicates a higher variety of correctly predicted reactants. Please note that diversity in predicted reactions is always desired, as it can enable the exploration of multiple synthetic options. With a more diverse set of options, chemists can choose the most suitable synthesis reactions based on specific requirements and constraints. This makes RLSynC a potentially preferable tool in synthetic design.

TABLE IV: Diversity@ N for Correct Synthon Completion

N	2	3	4	5	6	7	8	9	10
RSMILES	0.172	0.177	0.186	0.193	0.200	0.206	0.212	0.217	0.221
GraphRetro	0.197	0.205	0.212	0.217	0.222	0.227	0.231	0.234	0.237
G^2 Retro	0.194	0.202	0.209	0.216	0.222	0.229	0.236	0.243	0.249
RLSynC	0.193	0.205	0.231	0.243	0.251	0.256	0.260	0.265	0.272
imprv.(%)	-2.0	0.0	9.0*	12.0*	13.1*	11.8*	10.2*	9.1*	9.2*

The annotations in this table are the same as those in Table II.

3) *Validity Evaluation*: We also evaluate the validity of the completed synthons by the different methods. RLSynC and G^2 Retro always achieve 100% validity among its top- N predictions ($N \in [1, 10]$). This is because they enforces validity (Section IV-B), and completes synthons by adding atoms and bonds obeying valency rules. RSMILES can achieve on average 99.3% validity among top- N ($N \in [1, 10]$) predictions, and GraphRetro can achieve 98.4% validity. RSMILES formulates synthon completion as a sequence-to-sequence translation problem, so it cannot guarantee valency or the validity of the output strings. GraphRetro leverages a graph-based model of molecules, but uses a more relaxed set of valency rules when editing the molecular graphs.

B. Evaluation on Retrosynthesis Prediction

We also evaluate how RLSynC can contribute to retrosynthesis prediction. For RLSynC, we use the top-5 predicted reaction centers from G^2 Retro as given reaction centers and denote RLSynC in this method as RLSynC $_{G^2}$. G^2 Retro achieves the state-of-the-art performance on reaction center prediction (e.g., >96% accuracy [15]). For the other semi-template-based methods, we use their own reaction center prediction methods.

Since RLSynC can only perform synthon completion on two synthons, we limit RLSynC $_{G^2}$ to only those products for which G^2 Retro predicts a reaction center with exactly two synthons. To keep the comparison fair with other methods, we evaluate only on this subset of the test set, containing 2,607 products with two synthons predicted by G^2 Retro. Both template-free methods, including the template-free version of RSMILES [9] (denoted as R-p2r) and RetroFormer, and semi-template-based methods, including RetroPrime, RSMILES, GraphRetro and G^2 Retro, are compared. Due to space limits, we do not present their performance in terms of Diversity@ N .

1) *Correctness Evaluation*: Table V and VI present the performance in terms of MAP@ N and NDCG@ N , respectively, of all the methods for retrosynthesis prediction, that is, given a product, to predict the reactants. Table V shows that RLSynC $_{G^2}$ consistently outperforms the baselines for MAP@ N at $N \in$

[2, 10]. RetroFormer performs best among the baselines for MAP@N at $N \in [2, 10]$. For $N = 1$, RetroPrime outperforms all methods. RLSynC_{G²} significantly outperforms RetroFormer on 9 results, with the best improvement 14.0% at $N = 10$ and average improvement 8.8% over $N \in [2, 10]$. We observe that as N increases, the performance improvement from RLSynC_{G²} over other methods also increases, indicating that RLSynC_{G²} tends to predict more reactions that receive positive rewards.

TABLE V: MAP@N of Retrosynthesis Prediction

N	1	2	3	4	5	6	7	8	9	10
R-p2r	0.905	0.850	0.806	0.774	0.750	0.728	0.709	0.691	0.676	0.662
RetroFormer	0.890	0.851	0.817	0.790	0.768	0.744	0.725	0.707	0.689	0.670
RetroPrime	0.946	0.767	0.692	0.634	0.597	0.558	0.533	0.503	0.489	0.466
RSMILES	0.792	0.681	0.608	0.558	0.515	0.485	0.459	0.438	0.418	0.402
GraphRetro	0.896	0.835	0.789	0.748	0.708	0.673	0.641	0.611	0.582	0.555
G ² Retro	0.883	0.820	0.778	0.744	0.715	0.691	0.667	0.645	0.626	0.609
RLSynC _{G²}	0.899	0.882	0.863	0.844	0.824	0.810	0.796	0.784	0.774	0.764
impv.(%)	-5.0*	3.6*	5.6*	6.8*	7.3*	8.9*	9.8*	10.9*	12.3*	14.0*

The annotations in this table are the same as those in Table II.

TABLE VI: NDCG@N of Retrosynthesis Prediction

N	1	2	3	4	5	6	7	8	9	10
R-p2r	0.905	0.862	0.829	0.803	0.784	0.766	0.750	0.735	0.723	0.711
RetroFormer	0.890	0.860	0.834	0.813	0.795	0.777	0.762	0.747	0.733	0.718
RetroPrime	0.946	0.807	0.745	0.697	0.665	0.632	0.609	0.584	0.569	0.550
RSMILES	0.792	0.706	0.649	0.608	0.573	0.548	0.525	0.507	0.489	0.474
GraphRetro	0.896	0.849	0.813	0.781	0.751	0.724	0.699	0.675	0.651	0.630
G ² Retro	0.883	0.834	0.801	0.775	0.751	0.732	0.713	0.695	0.680	0.665
RLSynC _{G²}	0.899	0.886	0.872	0.857	0.843	0.831	0.821	0.811	0.802	0.794
impv.(%)	-5.0*	2.8*	4.6*	5.4*	6.0*	6.9*	7.7*	8.6*	9.4*	10.6*

The annotations in this table are the same as those in Table II.

RetroFormer embeds both the SMILES strings and molecular graphs of product molecules, and uses the embeddings to predict reaction center regions and generate reactant SMILES strings. By leveraging the rich information in such embeddings, RetroFormer is able to achieve good performance on MAP@N at $N \in [2, 10]$. RetroPrime first translates the SMILES strings of product into synthons, and then synthons into reactants. Both methods are trained to recover the unique ground-truth synthons and reactants in the training data, leading to superior MAP@1 performance. However, they do not consider any other possible synthons or reactants, and thus, fall short in generating multiple reactions, leading to worse performance on MAP@N at $N \in [2, 10]$.

In contrast to RetroFormer and RetroPrime, RLSynC_{G²} has the potential to discover new patterns by learning from random reactions and online interactions. In addition, RetroFormer and RetroPrime implicitly control the quality of top- N predictions through likelihood estimation, but RLSynC_{G²} takes a more direct approach. It uses the Q -function to directly evaluate the reward for a specific action (Equation 6 and 7), and then selects the actions with the best rewards so to optimize the quality of top- N predictions. As a result, RLSynC_{G²} improves the overall quality of top- N predictions and thus outperforms both RetroFormer and RetroPrime on MAP@N at $N \in [2, 10]$.

Among all the semi-template-based baselines (RetroPrime, RSMILES, GraphRetro and G²Retro), on average, GraphRetro and G²Retro perform the best – GraphRetro performs better on smaller N values, and G²Retro performs better on larger N values. As both GraphRetro and G²Retro are trained to recover ground-truth reactant molecules, they achieve comparable performance with RLSynC_{G²} on MAP@1 (0.896 vs 0.883 vs 0.899). However, RLSynC_{G²} outperforms GraphRetro and G²Retro in terms of MAP@N at $N \in [2, 10]$. As mentioned earlier, RLSynC_{G²} can directly optimize the overall quality of top- N predictions, resulting in more correct and higher-quality results among top- N predictions.

A similar trend can be observed in Table VI, which shows that RLSynC_{G²} consistently outperforms all the baselines on NDCG@N at $N \in [2, 10]$, with an average improvement of 6.9% over the best baseline and the best improvement 10.6% at $N = 10$. This demonstrates that RLSynC_{G²} tends to rank correct predicted reactions high, even when they come from different predicted reaction centers. Such capability allows chemists to sift out infeasible synthesis reactions, focusing on the most promising synthesis reactions instead. Please note that RLSynC_{G²} is trained on reactants from ground-truth reaction centers given in known reactions, not from predicted reaction centers. Thus, the results also demonstrate that RLSynC_{G²} can collaborate well with stand-alone reaction center predictors, enhancing its practical utility in synthetic design.

2) *Validity Evaluation*: We evaluate the validity of the predicted reactions from each retrosynthesis method. G²Retro and RLSynC_{G²} return only valid predicted reactions for retrosynthesis. Among the top-10 predictions, RetroFormer achieves an average 98.58% validity, RSMILES achieves 99.99%, R-p2r achieves 100.00%, GraphRetro achieves 99.77% and RetroPrime achieves 99.99%. RetroFormer, RSMILES, R-p2r and RetroPrime are all sequence-based methods; they do not strictly enforce the validity of their predicted results. GraphRetro adopts a flexible valency checking, resulting in a few molecules with rare valency of 5 for carbon atoms (usually 4). In our study, these molecules are considered invalid due to their rarity in drug molecules.

C. Evaluation on Data Augmentation

1) *Correctness Evaluation*: Fig. 3 and Fig. 4 present the performance in terms of MAP@N and NDCG@N from RLSynC over different online iterations of data augmentation, respectively, on synthon completion. Note that online data augmentation is determined by the continuity of performance improvement on the validation set (line 16 in Algorithm 1), and therefore, the performance on the test set may not be strictly improving over iterations. Even though, as Fig. 3 shows, with 8 online iterations of data augmentation, RLSynC is able to improve its MAP@N performance over all N values. For example, RLSynC improves its MAP@1 performance from 0.763 at iteration 0 (i.e., the initial model using only known and random reactions) to 0.927 after 8 iterations, that is, 21.5% improvement. Note that at iteration 6, the online data augmentation is switched from using only 1 new episode (line

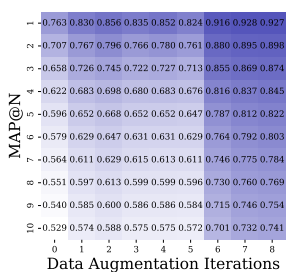


Fig. 3: MAP@ N over Data Augmentation Iterations



Fig. 4: NDCG@ N over Data Augmentation Iterations

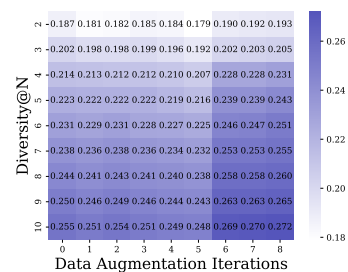


Fig. 5: Diversity@ N over Data Augmentation Iterations

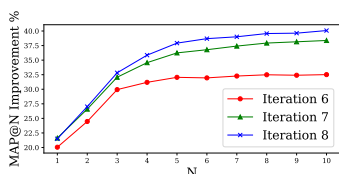


Fig. 6: MAP@ N Improvement from Top-5 Prediction Search

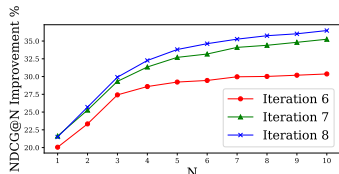


Fig. 7: NDCG@ N Improvement from Top-5 Prediction Search

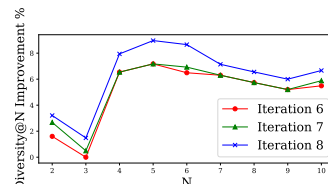


Fig. 8: Diversity@ N Improvement from Top-5 Prediction Search

10 in Algorithm 1) to the top-5 new episodes for each product, which significantly boosts performance.

Fig. 6 and Fig. 7 present the performance improvement in terms of MAP@ N and NDCG@ N from iterations 6, 7 and 8 over the initial model, respectively. From these figures, we see higher improvement from later iterations over the initial model. For example, in Fig. 6, the 8-th iteration can improve MAP@10 at 40.1%, whereas the 6-th iteration can improve MAP@10 at 32.5%. Note that the episodes generated for data augmentation in later iterations are derived from agents that have been trained on data from previous iterations. These episodes are more likely to contain correct reactions, and subsequent agents will benefit from training on these correct reactions, leading to better performance in later iterations.

2) *Diversity Evaluation*: Fig. 5 and Fig. 8 present the Diversity@ N for RLSynC across different data augmentation iterations. The best diversities result from iteration 8, with Diversity@10 as 0.272 as an example. Iterations 6, 7, and 8 provide large improvements to diversity. These iterations augment the dataset with 5 unique episodes per product, chosen by agents that have been trained for multiple iterations. In contrast, the first five iterations, which augment the dataset with only one episode per product, do not always improve Diversity@ N but improve NDCG@ N and MAP@ N .

VIII. DISCUSSION AND CONCLUSIONS

We developed RLSynC, a novel multi-agent reinforcement learning method with offline training and online data augmentation for synthon completion. RLSynC has two agents to complete the two synthons of a product into reactants. The two agents share the same action selection policy learned from known reactions, random reactions, and reactions that are generated and deliberately selected during the online data augmentation iterations. Using a forward synthesis prediction model as the reward function, RLSynC achieves superior

performance on synthon completion and for retrosynthesis prediction compared to the state-of-the-art methods.

In retrosynthesis prediction, how to evaluate predicted reactions automatically at scale is under-studied [31]. Existing methods compare the predictions with known reactions (i.e., ground truth) of products, and consider only the predictions that exactly match the ground truth to be correct. However, as demonstrated in Chen *et al* [15], many “incorrect” predictions can still be chemically possible, and may even represent more viable options. Thus, only comparing to the ground truth may underestimate the performance. Moreover, making the recovery of known reactions the only optimization objective may result in retrosynthesis prediction models that lack the ability to discover novel reactions.

RLSynC provides a new and versatile framework that can enable a more comprehensive evaluation paradigm. By using a reward function composed of multiple evaluation functions, it allows reaction evaluation with respect to the corresponding evaluation metrics, particularly when the reactions do not match the known reactions. Ideally, if high-throughput synthesis reactions can be conducted in laboratories over the predicted reactants, the reaction outcomes (e.g., yield) can be used as the reward. Even more importantly, RLSynC enables the exploration of new reactions that are not included in the ground truth, but are still feasible based on the reaction evaluation (i.e., the reward function), through online iterations of data augmentation. This feature makes RLSynC especially suitable for new reaction discovery purposes, and provide reactions with respect to specific evaluation metrics.

In future work, we will explore the following directions. We will generalize RLSynC for products with up to three reactants (i.e., up to three synthons; 100.00% of reactions in benchmark dataset). This can be done by allowing for three agents and empty synthons if there are fewer reactants. In these cases, the agents with empty synthons will only be able to choose

NOOP. We will also incorporate molecular graph representation learning within RLSynC so as to improve its power to represent and learn from synthon and product structures.

APPENDIX

We implement RLSynC in Python 3.8.13 using PyTorch 1.12.1, RDKit 2021.03.5, and gymnasium 0.27.0. For computing Q , we use a discount factor $\gamma = 0.95$ after considering $\{0.90, 0.95, 0.99\}$. In estimating Q , we use a four-layer feed-forward neural network with 4,096, 2,048, 1,024, and 1 output nodes on each respective layer. The input to the network $\mathbf{h}_{i,t}$, used 2,048-bit Morgan fingerprints of radius 2 without chirality. We used ReLU and 0.7 dropout between each layer, with no activation or dropout on the output. We explored dropout values of $\{0.1, 0.2, 0.3, 0.4, 0.5, 0.6, 0.7, 0.8\}$. We used the Adam optimizer with learning rate 10^{-4} after considering $\{10^{-3}, 10^{-4}, 10^{-5}\}$. to optimize the loss function in Equation 5 with a regularization coefficient of $\alpha = 10^{-5}$ after considering $\{10^{-4}, 10^{-5}\}$. During training, we iterate over batches of B products, where a training batch consists of $B \times T \times 2$ state-action pairs. For iterations 0 (initial model), 1, 2, 3, and 4 (data augmentation), we used $B = 10$. At iteration 5, as validation performance stabilized, we were able to see a small improvement by increasing B to 20. For iterations 5, 6, 7, and 8, we used $B = 20$.

For iterations 1, 2, 3, 4, and 5 for online data augmentation, we used one predicted reaction for each unique product in the training data to augment training data. For iterations 6, 7, and 8, we used top-5 predicted reactions ($N = 5$, $k = 3$ in Algorithm 2). When evaluating RLSynC, we produced top-10 predicted reactions for each product in the test set using our top- N search algorithm (Algorithm 2) with $N = 10$ and $k = 3$.

REFERENCES

- [1] B. Chen, C. Li, H. Dai, and L. Song, "Retro*: Learning retrosynthetic planning with neural guided a* search," in *Proceedings of the 37th International Conference on Machine Learning*, vol. 119 of *Proceedings of Machine Learning Research*, pp. 1608–1616, PMLR, 13–18 Jul 2020.
- [2] C. W. Coley, L. Rogers, W. H. Green, and K. F. Jensen, "Computer-assisted retrosynthesis based on molecular similarity," *ACS Cent. Sci.*, vol. 3, no. 12, pp. 1237–1245, 2017.
- [3] M. H. S. Segler and M. P. Waller, "Neural-symbolic machine learning for retrosynthesis and reaction prediction," *Chemistry - A European Journal*, vol. 23, no. 25, pp. 5966–5971, 2017.
- [4] H. Dai, C. Li, C. Coley, B. Dai, and L. Song, "Retrosynthesis Prediction with Conditional Graph Logic Network," in *Advances in Neural Information Processing Systems*, vol. 32, Curran Associates, Inc., 2019.
- [5] P. Seidl, P. Renz, N. Dyubankova, P. Neves, J. Verhoeven, J. K. Wegner, M. Segler, S. Hochreiter, and G. Klambauer, "Improving Few- and Zero-Shot Reaction Template Prediction Using Modern Hopfield Networks," *Journal of Chemical Information and Modeling*, vol. 62, pp. 2111–2120, May 2022.
- [6] I. V. Tetko, P. Karpov, R. Van Deursen, and G. Godin, "State-of-the-art augmented NLP transformer models for direct and single-step retrosynthesis," *Nature Communications*, vol. 11, p. 5575, Nov. 2020.
- [7] S.-W. Seo, Y. Y. Song, J. Y. Yang, S. Bae, H. Lee, J. Shin, S. J. Hwang, and E. Yang, "GTA: Graph Truncated Attention for Retrosynthesis," *Proceedings of the AAAI Conference on Artificial Intelligence*, vol. 35, pp. 531–539, May 2021.
- [8] Z. Tu and C. W. Coley, "Permutation Invariant Graph-to-Sequence Model for Template-Free Retrosynthesis and Reaction Prediction," *Journal of Chemical Information and Modeling*, vol. 62, pp. 3503–3513, Aug. 2022.
- [9] Z. Zhong, J. Song, Z. Feng, T. Liu, L. Jia, S. Yao, M. Wu, T. Hou, and M. Song, "Root-aligned SMILES: a tight representation for chemical reaction prediction," *Chemical Science*, vol. 13, pp. 9023–9034, Aug. 2022.
- [10] Y. Wan, C.-Y. Hsieh, B. Liao, and S. Zhang, "Retroformer: Pushing the Limits of End-to-end Retrosynthesis Transformer," in *Proceedings of the 39th International Conference on Machine Learning*, pp. 22475–22490, PMLR, June 2022. ISSN: 2640-3498.
- [11] C. Yan, Q. Ding, P. Zhao, S. Zheng, J. YANG, Y. Yu, and J. Huang, "RetroXpert: Decompose retrosynthesis prediction like a chemist," in *Advances in Neural Information Processing Systems*, vol. 33, pp. 11248–11258, Curran Associates, Inc., 2020.
- [12] C. Shi, M. Xu, H. Guo, M. Zhang, and J. Tang, "A Graph to Graphs Framework for Retrosynthesis Prediction," in *Proceedings of the 37th International Conference on Machine Learning*, pp. 8818–8827, PMLR, Nov. 2020. ISSN: 2640-3498.
- [13] X. Wang, Y. Li, J. Qiu, G. Chen, H. Liu, B. Liao, C.-Y. Hsieh, and X. Yao, "RetroPrime: A Diverse, plausible and Transformer-based method for Single-Step retrosynthesis predictions," *Chemical Engineering Journal*, vol. 420, p. 129845, Sept. 2021.
- [14] V. R. Somnath, C. Bunne, C. Coley, A. Krause, and R. Barzilay, "Learning Graph Models for Retrosynthesis Prediction," in *Advances in Neural Information Processing Systems*, vol. 34, pp. 9405–9415, Curran Associates, Inc., 2021.
- [15] Z. Chen, O. R. Ayinde, J. R. Fuchs, H. Sun, and X. Ning, "G2Retro as a two-step graph generative models for retrosynthesis prediction," *Communications Chemistry*, vol. 6, pp. 1–19, May 2023.
- [16] M. B. Smith, *Organic synthesis*. Elsevier, 2017.
- [17] J. You, B. Liu, R. Ying, V. Pande, and J. Leskovec, "Graph convolutional policy network for goal-directed molecular graph generation," in *Proceedings of the 32nd International Conference on Neural Information Processing Systems*, NIPS'18, (Red Hook, NY, USA), p. 6412–6422, Curran Associates Inc., 2018.
- [18] Z. Zhou, S. Kearnes, L. Li, R. N. Zare, and P. Riley, "Optimization of Molecules via Deep Reinforcement Learning," *Scientific Reports*, vol. 9, p. 10752, July 2019.
- [19] H. L. Morgan, "The Generation of a Unique Machine Description for Chemical Structures-A Technique Developed at Chemical Abstracts Service.," *Journal of Chemical Documentation*, vol. 5, pp. 107–113, May 1965.
- [20] C. Angermueller, D. Dohan, D. Belanger, R. Deshpande, K. Murphy, and L. Colwell, "Model-based reinforcement learning for biological sequence design," in *International Conference on Learning Representations*, 2020.
- [21] Z. Chen, M. R. Min, H. Guo, C. Cheng, T. Clancy, and X. Ning, "T-cell receptor optimization with reinforcement learning and mutation polices for precision immunotherapy," in *Research in Computational Molecular Biology* (H. Tang, ed.), (Cham), pp. 174–191, Springer Nature Switzerland, 2023.
- [22] J. S. Schreck, C. W. Coley, and K. J. M. Bishop, "Learning retrosynthetic planning through simulated experience," *ACS Central Science*, vol. 5, pp. 970–981, may 2019.
- [23] Z. Lan, Z. Zeng, B. Hong, Z. Liu, and F. Ma, "RCsearcher: Reaction Center Identification in Retrosynthesis via Deep Q-Learning," Jan. 2023. arXiv:2301.12071.
- [24] P. Schwaller, T. Laino, T. Gaudin, P. Bolgar, C. A. Hunter, C. Bekas, and A. A. Lee, "Molecular Transformer: A Model for Uncertainty-Calibrated Chemical Reaction Prediction," *ACS Central Science*, vol. 5, pp. 1572–1583, Sept. 2019.
- [25] F. Jaume-Santero, A. Bornet, A. Valery, N. Naderi, D. V. Alvarez, D. Proios, A. Yazdani, C. Bournez, T. Fessard, and D. Teodoro, "Transformer performance for chemical reactions: Analysis of different predictive and evaluation scenarios," *Journal of Chemical Information and Modeling*, vol. 63, pp. 1914–1924, mar 2023.
- [26] A. G. B. Richard S Sutton, *Reinforcement learning: An Introduction, 2nd edition*. MIT Press, 2018.
- [27] A. Nair, A. Gupta, M. Dalal, and S. Levine, "Awac: Accelerating online reinforcement learning with offline datasets," arXiv:2006.09359v6.

- [28] N. Schneider, N. Stiefl, and G. A. Landrum, "What's What: The (Nearly) Definitive Guide to Reaction Role Assignment," *Journal of Chemical Information and Modeling*, vol. 56, pp. 2336–2346, Dec. 2016.
- [29] A. Vaswani, N. Shazeer, N. Parmar, J. Uszkoreit, L. Jones, A. N. Gomez, L. Kaiser, and I. Polosukhin, "Attention is All you Need," in *Advances in Neural Information Processing Systems*, vol. 30, Curran Associates, Inc., 2017.
- [30] D. Bajusz, A. Rácz, and K. Héberger, "Why is tanimoto index an appropriate choice for fingerprint-based similarity calculations?," *Journal of Cheminformatics*, vol. 7, may 2015.
- [31] R. P. Philippe Schwalle, Vishnu H. Nair and T. Laino, "Evaluation metrics for single-step retrosynthetic models," in *Second Workshop on Machine Learning and the Physical Sciences (NeurIPS 2019)*, (Vancouver, Canada), 2019.